Open Access **Baghdad Science Journal** **P-ISSN: 2078-8665**
Published Online First: Suppl. November 2022 **2022, 19(6): 1551-1557** **E-ISSN: 2411-7986**

DOI: https://dx.doi.org/10.21123/bsj.2022.7409

Analysis of Fuel Burnup and Transmutations at High Burnup of Sodium Fast Breeder Reactor

***Nehal Mohamed*[1*]** ***Moustafa Aziz*[2]** ***M. El Ghazaly*[1]**
***Ibrahim Bashter*[1]**

[1]Physics Departement, Faculty of Science, Zagazig University, 44519 Zagazig, Egypt
[2]Department of Nuclear Safety Engineering, Egyptian Nuclear and Radiological Regulatory Authority, 7551 Nasr City, Cairo, Egypt
*Corresponding author: nehal.mo7md@gmail.com
E-mail addresses: moustafaaai@yahoo.com, ghazaly2000@yahoo.com, ibashter@hotmail.com

Received 11/5/2022, Accepted 27/7/2022, Published Online First 25/11/2022, Published 5/12/2022

This work is licensed under a Creative Commons Attribution 4.0 International License.

Abstract:

In this paper, the Monte Carlo N-Particle extended computer code (MCNP) were used to design a model of the European Sodium-cooled Fast Reactor. The multiplication factor, conversion factor, delayed neutrons fraction, doppler constant, control rod worth, sodium void worth, masses for major heavy nuclei, radial and axial power distribution at high burnup are studied. The results show that the reactor breeds fissile isotopes with a conversion ratio of 0.994 at fuel burnup 70 (GWd/T), and minor actinides are buildup inside the reactor core. The study aims to check the efficiency of the model on the calculation of the neutronic parameters of the core at high burnup.

Keywords: Fuel cycle, High burnup, Kinetic parameters, MCNP code, Neutronic calculations, Sodium Fast Reactor.

Introduction:

The Generation IV (Fourth Generation) International Forum (GIF) roadmap identifies fast reactors as a special, potentially sustainable energy source, especially in waste management and nuclear fuel optimization[1]. For 60 years of technical experience in related projects in many countries, sodium-cooled fast reactors (SFRs) are placed in a unique position among the various systems corroborative by GIF. Many countries have demonstrated significant technological advances in sodium-cooled fast reactors in design and operation terms[2]. The United States (US) Experimental Breeder Reactor (EBR) and Fast Flux Test Facility (FFTF), Russia's BN series reactors, Japan's Monju reactor, and France's Phénix prototype and commercial SuperPhénix have added more than 37 years of reactor operating experience in SFR technology[2].

The newest examples of sodium-cooled reactors are the recently linked to the net China Experimental Fast Reactor (CEFR)[3], India's prototype fast breeder reactor (PFBR)[4], and the Russian BN-800 reactor under construction[5]. For the Europe community, the "European Sustainable Nuclear Industrial Imitative" (ESNII) planned an industrial project called "Advanced Sodium Technological Reactor" (ASTRID) for many demonstration purposes. In addition to current fast reactor construction projects, many European countries are performing research programmes to develop pioneering fast reactor (GEN-IV) concepts.

The European Fast Sodium Reactor Community Project (CP-ESFR) is part of EURATOM's contribution to the GIF and seeks to create a common European framework to support fast sodium reactor technology. It was launched in the 7th EURATOM Framework Programme, with the aim of 24 European partners to create the technological basis for European fast sodium reactor plants (ESFR) to improve safety performance, resource efficiency, and cost-efficiency[6].

The design and safety parameter analysis of the world's nuclear reactors, in normal operation and under accident conditions needs continuous improvement of computational precision. In this

study, the Monte Carlo Neutron Transport Code MCNPX [7] was used to design an ESFR core model to analyze and evaluate a set of burnup-related properties. These include the axial and radial power distribution in the SFR core and the isotopic composition of the fuel. In addition, the performance characteristics at the start of cycle (BOC) and end of cycle (EOC) were investigated, considering the changes in the fuel isotopic composition during burnup[8]. The results obtained will serve as an updated analysis for further evaluation of fuel behavior and performance in the SFR core.

Reactor Description

The reactor core consists of inner and outer fuel zones. Each zone has a different fuel composition as shown in Fig. 1. There are 225 inner fuel assemblies and 228 outer fuel assemblies[9]. The reactor's control rod system is composed of two main devices: the Primary Control Rod (PCR) and the Secondary Control Rod (SCR). There are 24 SCR assemblies and 24 PCR assemblies[10]. In the designed model, the control assembly consists of a control rod located above the active zone, and the rest of the assembly is filled with sodium. Radial Reflector around the active core consists of 331 assemblies representing three rings around the core. The reflector consists of hexagonal blocks of a homogeneous mixture of 26% Na 74% EM10-like steel (% vol)[11]. Fig. 1, shows three radial zones in the horizontal layout of the core. The three radial zones are the inner core (in blue), the outer core (in orange), and the radial reflector (in yellow). There is one assembly of the reflector located in the center of the inner core. Furthermore, the PCR and SCR rods are dispersed into the two fuel zones.

There are 271 fuel pins in each fuel assembly. These pins are fixed in place by wire spacers and made of mixed oxide fuel (U, Pu)O_2 pellets. The cladding is formed from Oxide Strengthened steel (ODS)[11–13]. Fig. 2, shows the horizontal section of the fuel assembly and vertical section of the fuel pin. In the horizontal section of the fuel assembly, the blue color refers to the fuel pins, and the red color refers to the coolant, while the orange color indicates the structural materials.

The vertical section of the fuel pin consists of five zones (from the upper to bottom): the first zone is the axial reflector, the second zone is the upper gas plenum, the third zone is the Active core, the fourth zone is the axial reflector, and the fifth zone is the lower gas plenum with dimensions 80.4525 cm, 10.0566 cm, 100.566 cm, 30.1693 cm, and 89.9175 cm, respectively [13].

The active core is 100.55 cm long and is divided into equally five vertical zones with a length of 20.11 cm. Each vertical zone containes a variuos material composition, and the axial fuel composition has been altered to optimize and flatten axial flux and the axial power distributions[13–15].

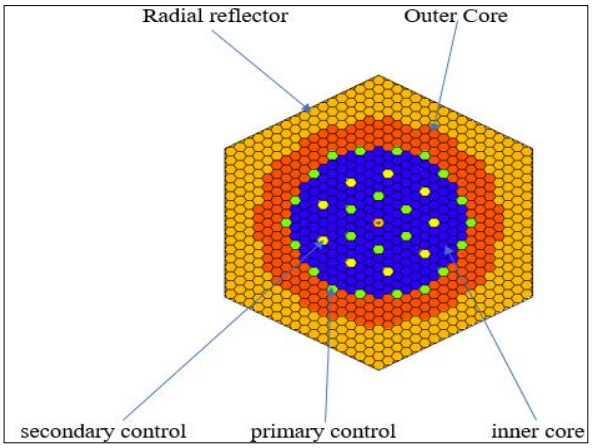

Figure 1. The horizontal section of the MCNP core model[9].

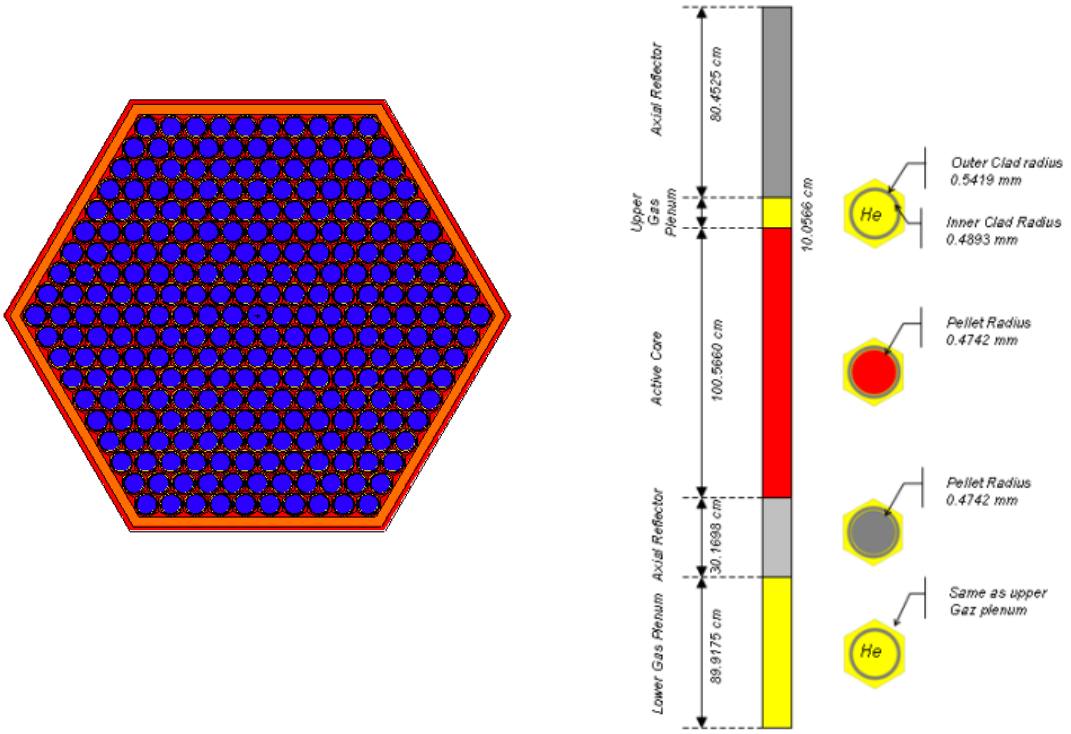

Figure 2. (a) The horizontal section of the fuel assembly, and (b) The vertical sections of the fuel pin models[9].

MCNPX computer model

Monte Carlo N-Particle Code (MCNP) is a general-purpose and a good computational instrument for Particle transport calculations. MCNPX (MCNP eXtended) is a Fortran90 (F90) Monte Carlo radiation transport computer code that transports many particles over a broad range of energies[7].

In aim work, a heterogeneous model of the reactor core was designed using MCNPX, as shown in Fig. 1[16]. Results are based on 12 million neutron histories. Calculations are based on the latest version of the ENDF library, which is already included in the MCNP library (ENDF/B-VII). At the burnup card, the fuel burns to 70 (Gwd/T) under normal operating conditions of the ESFR reactor. The cycle time is divided into 16-time steps.

Results and Discussions:

Table. I shows the comparison between MCNPX results and the reference as calculated by (serpent code)[17]. The reactor multiplication factor (K_{eff}) at (BOC) beginning of the cycle is 1.02863 and shows good agreement with the reference calculated by Serpent Code. The delayed neutron fraction (β_{eff}) for the reactor is 365 pcm which is less than the light water reactor because the fast reactor depends on plutonium as fuel which has a small fraction of delayed neutron fraction.

Table 1. Comparison of MCNPX and SERPENT for ESFR core

	Present model	Reference[17]	Difference
K_{eff} (Boc)	1.02863	1.02800	0.061%
β_{eff} (pcm)	365	360±8	1.38%
doppler coefficient (pcm)	-972	-982±9	1.01%
Control rod worth (pcm)	5385	5551±44	2.99%
Sodium void worth (pcm)	1706	1728±32	1.27%

The Doppler coefficient is calculated at fuel temperatures T1 and T2 and is chosen at 1200 ˚K and 1500 ˚K. The difference in results calculated from MCNP and reference for Doppler coefficient is 10 pcm or 1.01% in terms of relative error. It can be seen that the Doppler coefficient has a negative value which is attributed to the resonance cross-section of U-238. As the resonances of U-238 broadened, it reduced the self-shielding effect and resulted in negative feedback on reactivity.

The control rod worth is the reactivity difference between the two states: when all control rods are withdrawn from the core during normal operation and when all control rods are fully inserted. The difference in results calculated from MCNP and reference for Control rod worth is 166

pcm or 2.99%; when the control rods are inserted in the reactor core, the reactivity decrease (the neutron flux decreases) by absorbing neutrons[17].

The sodium void worth is calculated by replacing all sodium in the active core by void and equaling the reactivity difference between this state and the normal operation state. The sodium void worth is positive. This means that the reactivity increases due to the loss of coolant. Molten sodium works as a coolant for the reactor and also moderates neutrons when the core loses sodium and neutron moderation, neutron spectrum becomes more harder and shifts to higher neutron energy which is the more effective region in a fast reactor[17]. The difference in results calculated from MCNP and reference for Sodium void worth is 22 pcm or 1.27%.

Fig. 3, shows K_{eff} versus Burnup (GWd/T) for the present core model. The multiplication factor decreases with burnup due to fuel burnup and consumption. After 70 GWd/T, K_{eff} approach to unity.

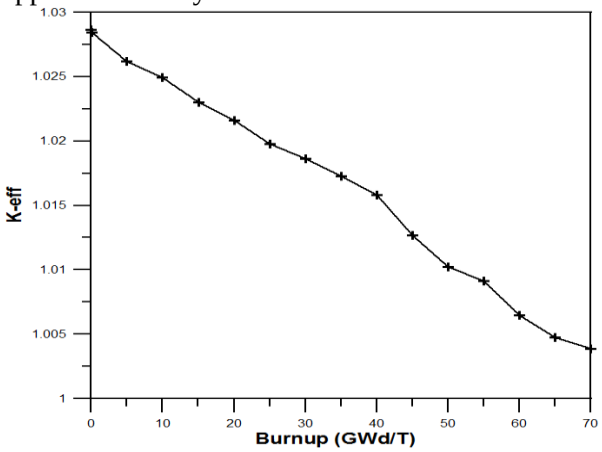

Figure 3. k_{eff} for the present core model with burnup (GWd/T).

Fig. 4, shows the fissile isotopes U-235 and Pu-241 versus core burnup (GWd/T) during core operation, and the results indicate that U-235 decreases from the beginning of the burnup 109 Kg up to 56 Kg at 70 (GWd/T) with the ratio of 51 %, which indicates U-235 consumption by more than 49%, while Pu-241 also decrease from 799 Kg at (t=0) to 627 Kg at 70 GWd/T with ratio 78 %, the consumption is 22 %.

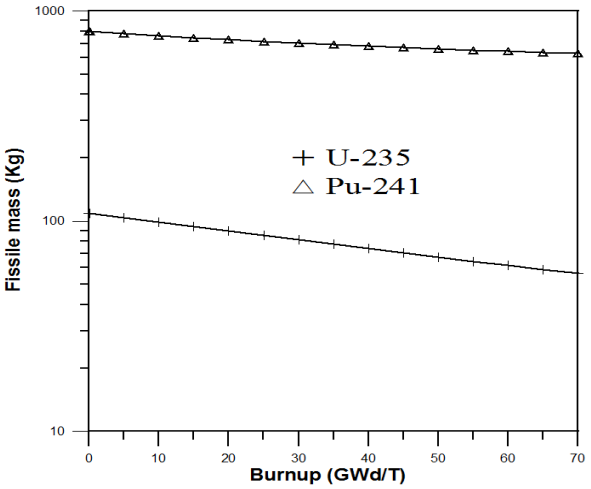

Figure 4. The total mass of U-235 (Kg) and Pu-241 for the present model with burnup (GWd/T).

Fig. 5, shows the total mass of Pu-239 (kg) versus core burnup (GWd/T) during reactor operation for the present model. The results indicate the Pu-239 (with initial mass 5627 Kg) increase during burnup and at 65 GWd/T start to decrease.

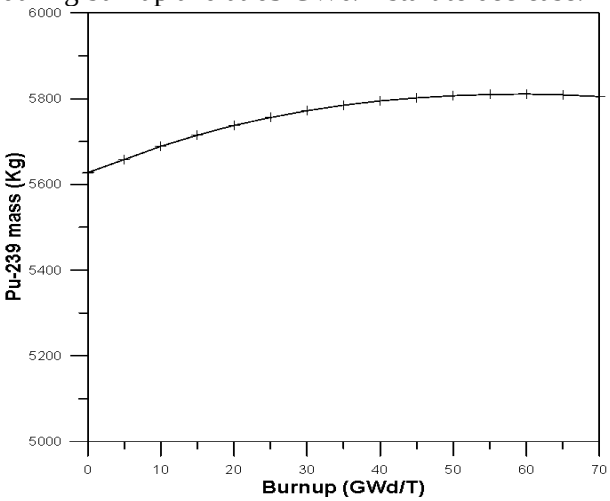

Figure 5. The total mass of Pu-239 (kg) versus core burnup (GWd/T) during reactor operation for the present model.

Fig. 6, shows conversion factor versus Burn up (GWd/T) for the core. The conversion factor increases up to 1.003 at 20 (GWd/T) then decreases to 0.9937 at 70 (GWd/T). The conversion factor increases with burnup due to the increase in mass of Pu-239 gradually due to its breeding from the fertile isotopes U-238. As shown in Fig. 4, the masses of U-235 and Pu-241 decrease during burnup through fission or transmutation by neutron capture. After 20 (GWd/T), the conversion factor started to decrease due to the slight decrease in mass of Pu-239 compared to the consumption of U-235 and Pu-241.

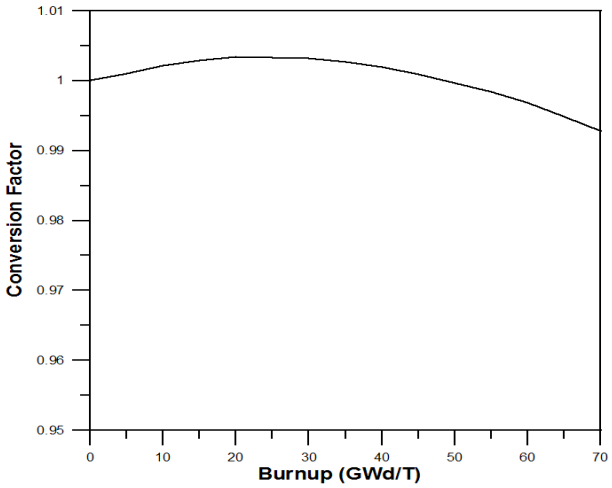

Figure 6. The conversion factor for the reactor core versus core burnup (GWd/T).

Fig. 7, shows Pu-238, Pu-240, and Pu-242 and total Plutonium isotopes versus core burnup (GWd/T). The results illustrated that Pu-238 and Pu-242 slightly decreased, while Pu-240 and total Pu isotopes slightly increased. [total Pu isotopes are the summation of all Plutonium isotopes, including Pu-239 and Pu-241, which appeared in the previous figures]. The total initial mass of Pu-238 for fresh fuel is 344.6 Kg and at 70 (GWd/T) is 258.8 Kg. The total initial mass of Pu-242 for fresh fuel is 1226 Kg and at 70 GWd/T is 1097 Kg. The total initial mass of Pu-240 for fresh fuel is 3524 Kg and at 70 (GWd/T) is 3810 Kg. The total initial mass of Pu isotopes for fresh fuel is 11521.2 Kg and at 70 (GWd/T) is 11598.2 Kg.

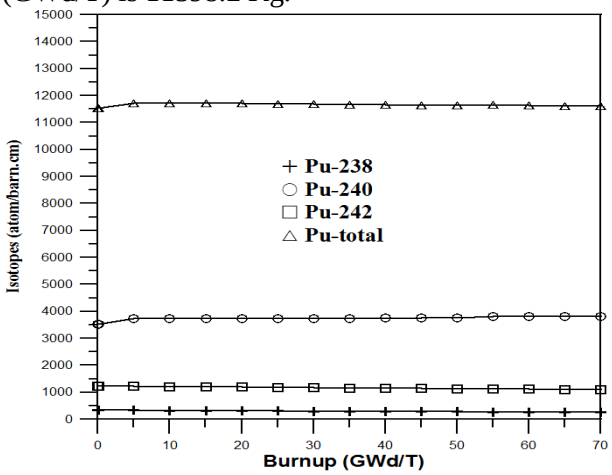

Figure 7. The total mass of Pu isotopes (Kg) for the present model with burnup (GWd/T).

Fig. 8, illustrates total mass of minor actinides build up during irradiation (Kg) [minor actinides represents summation of isotopes Np-237, Am-241, Am-242, Am-234, Cm-242, Cm-243, Cm-244, Cm-245, Cm-246, Cm-247] with Burn up (GWd/T) for the core during operation up to 70 GWd/T. The total mass of minor actinides increases gradually during burnup. This increase is mainly because of the transmutation of U-238 and Pu isotopes through neutron capture. The total initial mass of Np-237 for fresh fuel is 15.84 Kg and at 70 (GWd/T) is 34.24 Kg. The total initial mass of Am isotopes for fresh fuel is 247.39 Kg and at 70 (GWd/T) is 341.9 Kg. The total initial mass of Cm isotopes for fresh fuel is 23.46 Kg and at 70 GWd/T is 91.43 Kg. We find that this reactor builds minor actinides during operation.

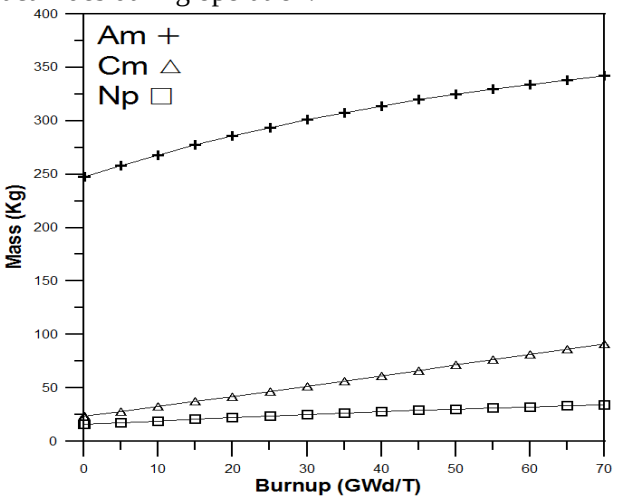

Figure 8. The total mass of minor actinides (Kg)with burnup (GWd/T).

Fig. 9, illustrates the radial power distribution across the core (1/6 of the core). The radial power is calculated at the third zone. The upper number represents the power at BOC, and the lower number refers to power at EOC. The maximum power is 1.567, and the minimum power is 0.107 at BOC. The maximum power is 1.069, and the minimum power is 0.219 at EOC.

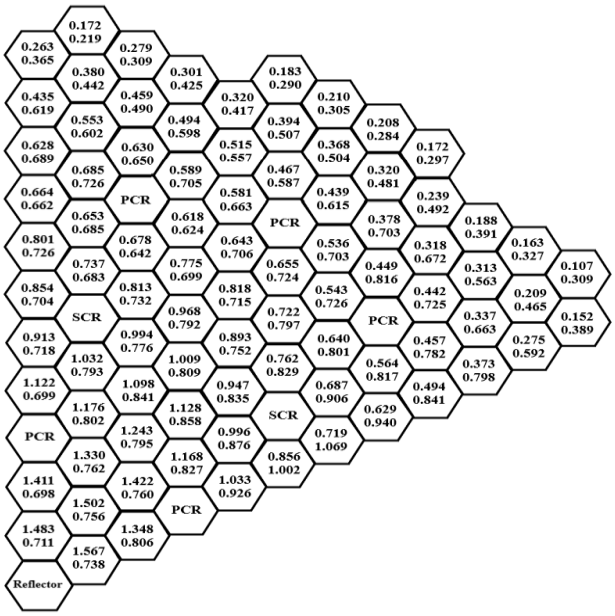

Figure 9. Radial power distribution across the core for the third zone.

Fig. 10, illustrates the axial power distribution across the axial core distance (cm) for the inner and outer core. The maximum power normalized is 1.4 and 1.2 for the inner and outer core, respectively.

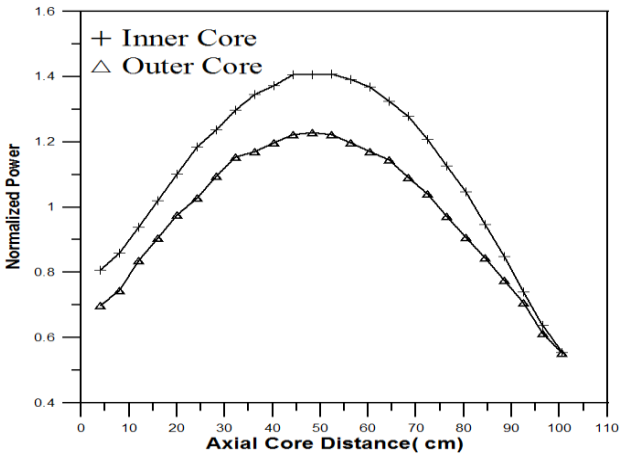

Figure 10. Axial power distribution normalized across the core.

Conclusions:

For the ESFR oxide-fuelled core, many fuel burnup-related parameters have been calculated using the Monte Carlo MCNPX computational code. These include the effective neutron multiplication factor (k_{eff}), conversion factor, radial and axial power distributions in the ESFR core, and the evolution of fuel composition inside the ESFR core. The axial and radial power have been evaluated for the beginning of the cycle (BOC) and at the end of the cycle (EOC), explicitly taking into account changes in core material composition during burnup. Also, the calculation by MCNPX shows an agreement with reference (SERPENT) for delayed neutrons fraction (β_{eff}), Doppler constant, control rod worth, and sodium void worth. By the end of the fuel cycle, the Pu-239 mass is increased, and the total fissile content of the core increases. Also, the conversion factor is higher than 1 during burnup. The obtained results showed that ESFR operates as a breeder with a conversion ratio of 0.994.

Acknowledgements:

The authors acknowledge the computational support provided by the Supercomputing Facility of the Bibliotheca Alexandrina, Egypt.

Authors' declaration:

- Conflicts of Interest: None.
- We hereby confirm that all the Figures and Tables in the manuscript are mine ours. Besides, the Figures and images, which are not mine ours, have been given the permission for re-publication attached with the manuscript.
- Ethical Clearance: The project was approved by the local ethical committee in Zagazig University.

Authors' contributions statement:

N.M. and M.A. designed the model and the computational framework and analyzed the data. N.M. and I.B. carried out the implementation. N.M. performed the calculations. N.M. and M.A. wrote the manuscript with input from all authors. M.A., M.E., and I.B. conceived the study and were in charge of overall direction and planning.

References

1. Merk B, Litskevich D, Bankhead M, Taylor RJ. An innovative way of thinking nuclear waste management – Neutron physics of a reactor directly operating on SNF. PLOS ONE. 2017. Jul; 12(7): 1-19.
2. Hill RN, Therios I, Cipiti BB, Kim HD. Sodium-Cooled Fast Reactor Proliferation Resistance and Physical Protection White Paper. NNSA. 2020 Oct; 12214: 1-25. Available from: https://www.osti.gov/servlets/purl/1710232/
3. Tran TQ, Lee D. Neutronic simulation of the CEFR experiments with the nodal diffusion code system RAST-F. Nucl Eng Technol. 2022; 54(7): 2635–2649.
4. Saha U, Devan K, Bachchan A, Pandikumar G, Ganesan S. Neutron radiation damage studies in the structural materials of a 500 MWe fast breeder reactor using DPA cross-sections from ENDF / B-VII.1. Pramana – J Phys. 2018; 90(4): 46-61.
5. Maslov NV, Grishanin EI, Alekseev PN. The possibility of improving inherent safety BN-800 by the use of fuel assembly with (U, Pu)C microfuel. Izv vuzov Yad Energ. 2019 Mar; 2019(1): 71–84.
6. Rineiski A, Mériot C, Marchetti M, Krepel J, Coquelet-Pascal C, Tsige-Tamirat H, et al. ESFR-SMART Core Safety Measures and Their Preliminary Assessment. J Nucl Eng Radiat Sci. 2021; 8(1): 1130-1140.
7. Pelowitz DB. MCNPX User's Manual Version 2.7.0. Los Alamos Sci. 2011.
8. Galfas AA, Fayyadh IK, Hassan HA, Aziz AK. Study of Reactivity Effect on Reactor Power by Using the Neutronic- Thermohydrolic Coupling. Baghdad Sci J. 2012 Sep; 9(3): 459–465.
9. Fridman E, Velarde FA, Otero PR, Tsige-Tamirat H, Antonio J, García-Herranz N, et al. Neutronic Analysis of the European Sodium Fast Reactor: Part I—Fresh Core Results. J Nucl Eng Radiat Sci. 2021 Jul; 8(1).011301: 1056-1066. https://doi.org/10.1115/1.4048905
10. Abbood AS, Ibraheem IJ. Synthesis of Carbon Nano Rods from Plastic Waste (PP) Using MgO AS A Catalyst. Baghdad Sci J. 2020 Jun; 17(2): 609-613.
11. Fridman E, Velarde FA, Otero PR, Tsige-Tamirat H, Antonio J, García-Herranz N, et al. Neutronic

Analysis of the European Sodium Fast Reactor: Part II—Burnup Results. J Nucl Eng Radiat Sci. 2021 Jul; 8(1). 011302: 1067-1077. DOI: https://doi.org/10.1115/1.4048765
12. Davies U, Margulis M, Shwageraus E, Fridman E, García-Herranz N, Antonio J, et al. Evaluation of the ESFR end of cycle state and detailed analysis of spatial distributions of reactivity coefficients. EPJ Web Conf. 2021; 247: 02001. DOI:10.1051/epjconf/202124702001
13. Mohamed N, Aziz M, Bashter I. Studying the effect of assembly homogenization on fuel burn-up for a sodium-cooled fast breeder reactor. J Korean Phys Soc. 2021 Jul; 79(2): 160–167.
14. Antonio J, García-Herranz N, Krepel J, Margulis M, Baker U, Shwageraus E, et al. Decay Heat Characterization for the European Sodium Fast Reactor. J Nucl Eng Radiat Sci. 2022; 8(1): 1051-1060.
15. Stauff NE, Kim TK, Taiwo TA, Buiron L, Rimpault G, Lee YK, et al. Evaluation of the OECD/NEA/SFR-UAM Neutronics Reactivity Feedback and Uncertainty Benchmarks. IAEA. 2017; 49(44): 149-160.
16. Fensin ML, Hendricks JS, Anghaie S. The Enhancements and Testing for the MCNPX 2.6.0 Depletion Capability. Nucl Technol. 2010 Apr; 170(1): 68–79.
17. Nhan MN, Jo TY, Lee HS, Cherezov A, Lee DJ. Whole-core Monte Carlo Analysis of MOX-3600 Core in NEA-SFR Benchmark Using MCS Code. Proceedings of the KNS Fall Meeting . 2018.

تحليل احتراق الوقود وتحويلاته عند الاحتراق العالي لمفاعل الصوديوم السريع

نهال محمد[1] مصطفي عزيز[2] محمود الغزالي[1] إبراهيم بشطر[1]

[1] قسم الفيزياء، كلية العلوم، جامعة الزقازيق، ص.ب.44519 الزقازيق، مصر
[2] قسم هندسة الأمان النووي، الهيئة المصرية العامة للرقابة النووية والإشعاعية، ص.ب.7551 مدينة نصر، القاهرة، مصر

الخلاصة:

في البحث الحالي تم استخدام برنامج حاسوبي بطريقة مونتي كارلو الموسع لـ لتصميم نموذج للمفاعل السريع الأوروبي المبرد بالصوديوم. قمنا بدراسة عامل الضرب، عامل التحويل، كسر النيوترونات المتأخرة، ثابت دوبلر، قيمة قضيب التحكم ، قيمة فراغ الصوديوم، كتل النوى الثقيلة الرئيسية ، توزيع القدرة الشعاعية والمحورية عند الاحتراق العالي. أظهرت النتائج أن المفاعل يولد نظائر انشطارية بمعدل تحويل 0.994 عند 70 (GWd/T) احتراق الوقود وتتراكم الأكتينيدات الصغيرة داخل قلب المفاعل. تهدف الدراسة إلى التحقق من كفاءة النموذج في حساب البارامترات النيوترونية للنواة عند الاحتراق العالي.

الكلمات المفتاحية: دورة الوقود ,الاحتراق العالي, المعاملات الحركية, كود مونتي كارلو, الحسابات النيوترونية, مفاعل الصوديوم السريع.